

Figure 2. The three building blocks of **1a**: (a, left) the hexanuclear Mo(V)-ligand moiety $\{\text{Mo}^{\text{V}}_6\text{O}_{22}(\text{HL})\}$ (**1b**) of which there are four in the molecular anion; (b, center) the tetranuclear Mo(V)/Mo(VI)-ligand unit $\{\text{Mo}^{\text{V}}_2\text{Mo}^{\text{VI}}_2\text{O}_{15}(\text{HL})\}$ (**1c**) of which there are three in the molecular anion; (c, right) the central hexanuclear Mo(V) core $\{\text{Mo}_6\text{O}_{24}\}$ (**1d**).

structural unit, of which there are three present in **1a**, consists of the tridentate ligand bridging a triangular core of one Mo(V) and two Mo(VI) centers (**1c**); the Mo(V) site is in turn associated through edge-sharing by two oxo groups with an exocyclic Mo(V) unit, with the usual short Mo–Mo interaction. Finally, there is a six-membered Mo(V) ring $\{\text{Mo}_6\text{O}_{24}\}$ of edge-sharing octahedra with alternating short–long Mo–Mo distances (**1d**). The ring **1d** provides the central core of the cluster, with the four hexanuclear (**1b**) and three tetranuclear (**1c**) units disposed about it through edge- and corner-sharing of octahedral motifs.

The tetranuclear units **1c** project outward from the cluster like the arms of a grapple to produce an open cavity. The sides of the cavity are defined by the octahedra of the central ring **1d** and the *cis*-dioxo groups of the six Mo(VI) sites. The $[\text{Na}(\text{H}_2\text{O})_3]^+$ moiety is located within this cavity.

The structural parameters and valence sum calculations¹² identify the anion as a mixed-valence Mo(V)/Mo(VI) species. The 36 Mo(V) sites are readily identified by the presence of 18 Mo(V)/Mo(VI) binuclear units with short Mo–Mo distances. The six Mo(VI) sites exhibit terminal *cis*-dioxo coordination and the absence of short Mo–Mo distances as unique structural characteristics. Since the overall anion charge of the unit $[\text{Na}(\text{H}_2\text{O})_3\text{Mo}_{42}\text{O}_{109}(\text{HL})_7]^{22-}$ is 22– and there are four Na^+ cations, one $(\text{Et}_4\text{N})^+$ cation, and two $(\text{Me}_3\text{NH})^+$ cations associated with the structure, there must be 15 H^+ per formula unit to balance the charge. The 15 protonation sites are readily identified from the metric parameters of **1a** as triply-bridging oxo groups: the oxo groups which connect the ring **1d** to the central **1b** fragment (O24 type), the central oxo groups of each of the ligand-bridged triangular cores of the four **1b** units (O4 type) and the three **1c** units (O122 type), the oxo groups linking the central ring **1d** to the **1c** units (O96, O97, O99) and two of the six triply-bridging oxo groups which are involved in linking octahedra belonging to each of the three structural motifs (O25 type) (13). It is noteworthy that the remaining four triply-bridging oxo groups of this type exhibit close contacts to Na^+ cations of the lattice to compensate for the absence of a proton. These four Na^+ cations are imbedded in four of six cavities formed by the fusion of the three peripheral **1b** subunits with the central **1b** subunit and the **1c** fragments.

While the mechanism of compound formation in the hydrothermal synthesis of **1** remains obscure, factors such as pH, the reducing nature of the medium, and templating cations are significant. Thus, **1** could only be isolated in the presence of Na^+ at low pH. While other cations do yield polyoxoalkoxomolybdate clusters under similar conditions, the compositions are quite

different; we are currently investigating the structures of these species.

Acknowledgment. This work was supported by NSF Grant CHE9119910.

Supplementary Material Available: Tables of crystal data and experimental conditions, atomic positional parameters, bond lengths, bond angles, and anisotropic temperature factors for the X-ray study of **1**, polyhedral views of the structure, and a valence sum discussion (31 pages); tables of calculated and observed structure factors for **1** (71 pages). Ordering information is given on any current masthead page.

Fourier-Transform EPR Investigation of Photogenerated Radical Anions of C_{60} in Solution

M. Ruebsam and K.-P. Dinse*

*Institute for Physical Chemistry
Technical University Darmstadt
D-6100 Darmstadt, Germany*

M. Plueschau

*Physics Institute, University Dortmund
D-4600 Dortmund, Germany*

J. Fink

*Kernforschungszentrum Karlsruhe, INFP
D-7500 Karlsruhe, Germany*

W. Kraetschmer and K. Fostiropoulos

*MPI fuer Kernforschung
D-6900 Heidelberg, Germany*

C. Taliani

*Instituto di Spettroscopia Molecolare
I-40126 Bologna, Italy*

Received May 27, 1992

The new phases of carbon, and in particular its most symmetrical representative C_{60} , are attracting intense attention. Although ^{13}C NMR has been used for an unambiguous identification, EPR experiments have been less successful for a characterization of its paramagnetic derivatives. Early attempts to produce C_{60} -related doublet radicals either by photolysis,¹ by alkali metal reduction,²

(12) Brown, I. D. In *Structure and Bonding in Crystals*; O'Keefe, M., Navrotsky, A., Eds.; Academic Press: New York, 1981; Vol. 2, p 1.

(13) The detailed arguments for these assignments are presented in the supplementary material.

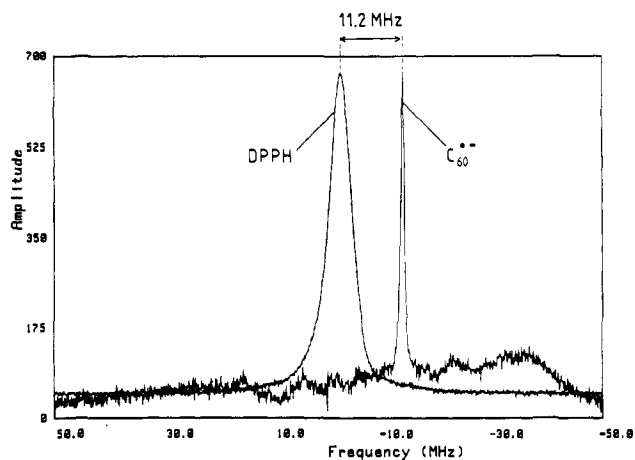


Figure 1. FT-EPR spectrum obtained by laser excitation (580 nm) of C_{60} in toluene. The signal shown was taken at 300 K and using a delay of 800 ns. Positive amplitude corresponds to an absorptive signal. From $\Delta\nu = -11.2$ (1) MHz and $\nu_0 = 9.054$ GHz a g -factor shift $\Delta g = -2.48 \times 10^{-3}$ relative to $g(\text{DPPH}) = 2.0037$ is obtained, leading to $g(C_{60}^{\cdot-}) = 2.0012$ (1), the accuracy being determined by the DPPH value.

by γ irradiation,³ by electrochemistry,⁴ or by trapping in molecular sieves⁵ invariably either led to several species which could not be assigned unambiguously or to unstable compounds, which had to be stabilized by trapping in frozen solvents. Only recently, Greaney and Gorun⁶ reported about the generation of apparently long-lived monoanions radical of C_{60} and C_{70} by controlled-potential coulometry in $\text{CH}_2\text{Cl}_2/\text{toluene}$ with Bu_4NPF_6 as electrolyte.

As an alternative to electrochemical generation, it is possible to produce paramagnetic C_{60} derivatives by photoinduced charge separation. Instead of utilizing the method of UV-photolysis of added donor molecules for the production of $C_{60}^{\cdot-}$,¹ we studied the possibility of charge separation by direct excitation of C_{60} with 580-nm photons, thus precluding excitation of solvent molecules or other organic impurities.

As was demonstrated for various radicals, FT-EPR in combination with laser excitation is the ideal method for the investigation of short-lived paramagnetic reaction products.⁷ We investigated dilute ($c \approx 10^{-3}$ M) solutions of C_{60} in thoroughly degassed toluene sealed off on a high-vacuum line. As is shown in Figure 1, a narrow EPR line ($g = 2.0012$ (1)) could be observed at room temperature. Its line width (FWHM) of 700 (50) kHz is similar to the quoted value (peak-to-peak) of 0.02 mT.² The g -factor was determined by comparison with the resonance position of solid DPPH. Samples of C_{60} and C_{60}/C_{70} mixtures of different origin were used, all of which resulted in the same transient EPR signal.

Using triplet-triplet absorption, the presence of triplet state $^3C_{60}$ in solution with a lifetime well above several microseconds has been established.^{8,9} For an assignment of the transient EPR signal we therefore had to consider the possibility that it might originate from $^3C_{60}$, as suggested by Closs et al.¹⁰ The signature

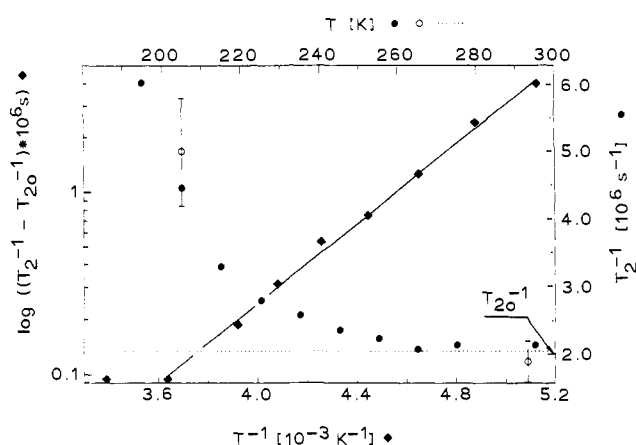


Figure 2. Spin dephasing rate T_2^{-1} as a function of temperature. T_2 is derived from the exponential decay constant of the FID. T_1 (open circle) was found identical within measurement accuracy. The deperature-activated part of T_2^{-1} is depicted in a semilog plot vs $1/T$ for a determination of ΔE .

of laser-generated $^3C_{60}^{\cdot-}$ would be an intensity buildup with the time constant of the apparatus function ($t \approx 30$ ns⁷), independent of temperature. Varying the time delay between the laser pulse and the $\pi/2$ -microwave pulse, the buildup and decay kinetics was determined for 205 and 300 K. The signal increases multiexponentially ($\tau_1 \approx 30$ ns, $\tau_2 \approx 1.2$ μs , and 670 ns for 205 and 300 K, respectively) and decays also at least biexponentially. The presence of an additional rise time much larger than the apparatus time constant which is also temperature dependent is at variance with an assignment of the observed signal to $^3C_{60}$.

From the analysis of CIDEP processes,⁷ one has to expect contributions from at least two different mechanisms of spin polarization, i.e., either by direct transfer of triplet spin polarization (TM) or by the radical-pair mechanism (RPM), both of which characterized by different time constants. The sign of both contributions will be identical and absorptive in our case. As was shown by Wasielewski et al.,¹³ intersystem crossing leads to a predominant population of the lowest zero-field level(s), thus generating an absorptively-polarized triplet precursor. A Boltzmann-type RPM polarization is generated if the charge transfer occurs from a triplet state and if the corresponding cation radical has a higher g -factor than the actually observed radical. Both conditions seem to be fulfilled. The two time constants mentioned above can be identified with the charge-transfer rate and the triplet spin relaxation time.⁷ Details of the analysis will be presented elsewhere.

Using a π - $\pi/2$ pulse sequence, it was proven that the signal is absorptive at all times, and that the width of the perfect Lorentzian line was determined by T_1 , i.e., $T_1 = T_2$. For an interpretation, the temperature dependence of T_2 was measured from 190 to 300 K. As is shown in Figure 2, T_2^{-1} increases monotonically toward lower temperatures. It was verified for 205 K, $T_1 = T_2$ still holds. This is indicative for a relaxation process in the limit $\omega_0\tau_c \ll 1$. From this, dominant contributions from electron-nuclear-dipole interaction or from g -factor anisotropy are excluded, because the estimated rotational correlation time $\tau_r \approx 0.8$ ns $\gg \omega_0^{-1}$ in toluene even at 300 K.¹² Furthermore, spin-rotational interaction is also precluded, because $T_1^{-1}(\text{SR}) \sim \tau_r^{-1}$ ¹² and its contribution would be decreasing at lower temperatures. We therefore conclude that the observed relaxation behavior is indicative for thermally-activated population of

(1) Krusic, P. J.; Wasserman, E.; Parkinson, B. A.; Malone, B.; Holler, E. R., Jr.; Keizer, P. N.; Morton, J. R.; Preston, K. P. *J. Am. Chem. Soc.* **1991**, *113*, 6274.

(2) Kukolich, S. G.; Huffman, D. R. *Chem. Phys. Lett.* **1991**, *182*, 263.

(3) Kato, T.; Matsui, Y.; Suzuki, S.; Shiromaru, H.; Yamauchi, K.; Achiba, Y. *Chem. Phys. Lett.* **1991**, *186*, 35.

(4) Allemand, P. M.; Srdanov, G.; Koch, A.; Khemani, K.; Wudle, F. J. *Am. Chem. Soc.* **1991**, *113*, 2780.

(5) Keizer, P. N.; Morton, J. R.; Preston, K. F.; Sudgen, A. K. *J. Phys. Chem.* **1991**, *95*, 7117.

(6) Greaney, M. A.; Gorun, S. M. *J. Phys. Chem.* **1991**, *95*, 7142.

(7) Kroll, G.; Plueschau, M.; Dinse, K.-P.; van Willigen, H. *J. Chem. Phys.* **1990**, *95*, 8709 and references therein.

(8) Arbogast, J. W.; Darmann, A. P.; Foote, C. S.; Rubin, Y.; Diederich, F. N.; Alvarez, M. M.; Anz, S. J.; Whetten, P. L. *J. Phys. Chem.* **1991**, *95*, 11.

(9) Kajii, Y.; Nakagawa, T.; Suzuki, S.; Achiba, Y.; Obi, K.; Shibuya, K. *Chem. Phys. Lett.* **1991**, *186*, 100.

(10) Closs, G. L.; Gantan, P.; Zhang, D.; Krusic, P. J.; Hill, S. A.; Wasserman, E. Preprint.

(11) Unfortunately, the most direct method for discrimination of $S = 1/2$ and $S = 1$ species by measuring the change of the rabi frequency by $\sqrt{2}$ originating from an increase of the matrix element of S_x , could not be utilized here, because of frequency-degenerate $| -1 \rangle$ to $| 0 \rangle$ and $| 0 \rangle$ to $| +1 \rangle$ transitions in the case of vanishing ZFS. One of us (K.-P.D.) is indebted to M. Mehring for enlightening discussions and to E. Wasserman for his insistent questions.

(12) Plato, M.; Lubitz, W.; Moebius, K. *J. Phys. Chem.* **1981**, *85*, 1202.

(13) Wasielewski, M. R.; O'Connell, M. P.; Lykke, K. R.; Pellin, M. J.; Gruen, D. M. *J. Am. Chem. Soc.* **1991**, *113*, 2774.

close-lying electronic states, originating either from Jahn-Teller distortion or by solvent-induced lifting of the 3-fold orbital degeneracy of the mononegative anion. In this model, $\tau_c \sim \exp(-\Delta E/kT)$ denotes the average time of the radical in its ground state, ΔE denoting the energy difference of the electronic singlet to the remaining doublet. The resulting $J(\omega) \sim \tau_c/(1 + \omega^2\tau_c^2)$ leads to $T_2^{-1} = T_1^{-1} \sim \exp(\Delta E/kT)$ in the limit $\omega_0^2\tau_c^2 \ll 1$. The anticipated thermally-activated contribution to T_2 can be used for a determination of ΔE , after subtracting the high-temperature width of 700 kHz, as is shown in Figure 2. It is tempting to correlate this value of $\Delta E = 450 \text{ cm}^{-1}$ with a value, deduced from the g -factor shift relative to the free electron value.³ Following the arguments of Kato et al., we obtain $\Delta E' = 210 \text{ cm}^{-1}$. Considering the various assumptions used in ref 3, this factor-of-two agreement is very satisfactory.

Various questions still remain unanswered. Firstly, in agreement with all other EPR results, no ¹³C satellites have been observed. However, using a simple Karplus-Fraenkel estimate, $a(C^{13}) \approx (-10) \times 2.8/60 \text{ MHz} = -460 \text{ kHz}$ is obtained, just at the resolution limit of our experiment. Secondly, the postulated charge separation also leads to the formation of a cation radical, which was also not visible. A possible explanation might be the generation of a radical adduct with unresolved hfs, therefore not detectable with a $\pi/2$ excitation. Search with an echo sequence, however, was also unsuccessful, excluding radicals with $T_2 \geq 500 \text{ ns}$.

Acknowledgment. The FT-EPR spectrometer was financed partially by a grant of the Deutsche Forschungsgemeinschaft (Di 182/3). One of us (C.T.) wants to thank Ms. S. Rossini for technical assistance.

Registry No. C₆₀, 99685-96-8; C₆₀^{•-}, 111138-12-6.

Polymer-Supported Synthesis of 2,5-Disubstituted Tetrahydrofurans

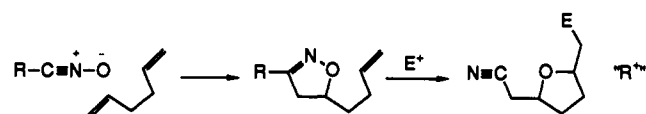
Xenia Beebe, Neil E. Schore,* and Mark J. Kurth*¹

Department of Chemistry
University of California, Davis
Davis, California 95616

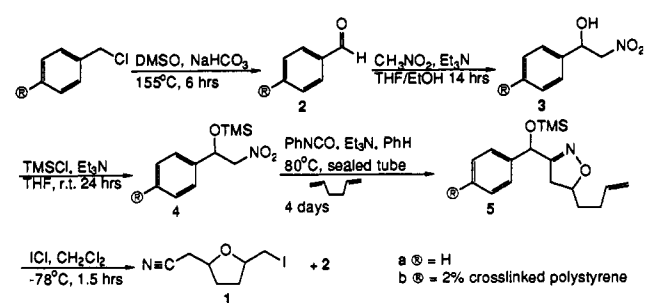
Received July 27, 1992

Polymer-supported synthesis is an important tool for the development of new synthetic strategies in organic chemistry,² and the literature associated with polymer-supported reagents and catalysts is extensive.³ Merrifield's pioneering work in the area of polymer-supported polypeptide synthesis⁴ delineated many of the benefits of a polymer-supported synthetic strategy, with the most obvious being ease of workup and ease of product isolation. In addition, side product formation is often minimized when the reactive species is covalently attached to a polymer support.⁵ Intrigued by these potential advantages, we set out to explore the application of polymer-supported reactions in multistep synthetic organic chemistry and describe herein a polymer-supported strategy which improves upon an α,ω -diene \rightarrow cyclic ether protocol recently reported from our laboratories.⁶ Thus, the targeted

Scheme I



Scheme II



process involves the five-step synthesis of 2,5-disubstituted tetrahydrofurans via a tandem 1,3-dipolar cycloaddition/electrophilic cyclization sequence.

2,5-Disubstituted tetrahydrofurans are important structural elements in many polyether antibiotics⁷ and, as a compound class, have proven to be synthetically challenging molecules.⁸ In earlier work, we demonstrated that the tandem process outlined in Scheme I provides useful entry to such compounds. Unfortunately, the protocol as originally developed suffers one major drawback when carried out under normal homogeneous conditions.⁹ That is, it utilizes an α,ω -diene substrate in the 1,3-dipolar cycloaddition step and thus requires selective monoaddition of the nitrile oxide to this dipolarophile. However, in solution a second nitrile oxide is free to react with the remaining terminal alkene, leading to the undesired product of bis 1,3-dipolar cycloaddition. As previously reported, this bis addition can be suppressed by using the diene in a 10-fold excess. Clearly as the α,ω -diene becomes more complex and/or expensive, this solution to the bis-addition problem becomes less and less attractive.

As an approach to solving this problem, we considered potentially beneficial the partial isolation that might be achieved by covalent attachment of the nitrile oxide moiety to an insoluble polymer matrix. The terminal alkene remaining after isoxazole formation would be less accessible to another polymer-bound nitrile oxide, which would then have a higher probability of reacting with remaining diene. The latter could then be used in smaller excess. An additional benefit of the polymer-supported method is that the iodocyclization reaction was envisioned to liberate exclusively the target cyclic ether. This transformation also would simultaneously regenerate a functionalized polymer, which could be recycled through this synthetic scheme.

The planned synthesis thus had two polymer prerequisites: (1) straightforward generation of a polymer-bound nitrile oxide precursor and (2) incorporation of cation-stabilizing functionality (in the polymer-bound R group) to facilitate the electrophilic cyclization reaction. We felt it most convenient to meet these requirements in the context of the functionality accessible from Merrifield's polystyrene resin.¹⁰ The approach outlined in Scheme II appeared to be especially attractive since the final cyclization step would regenerate the initial polymer-bound aldehyde for potential recycling. The chemistry presented in Scheme II was first investigated using conventional solution-phase methods (i.e., encircled R = H) and employing a 10-fold excess of α,ω -diene in the critical cycloaddition step. We thus obtained the final product, 2-(cyanomethyl)-5-(iodomethyl)tetrahydrofuran (1), as

(1) Sloan Foundation Fellow (1987-1991) and NIH RCDA recipient (1989-1994; EC00182).

(2) (a) Xu, Z.-H.; McArthur, C. R.; Leznoff, C. C. *Can. J. Chem.* **1983**, *61*, 1405. (b) Fréchet, J. M. J. *Tetrahedron* **1981**, *37*, 663. (c) Leznoff, C. C. *Acc. Chem. Res.* **1978**, *11*, 327. (d) Crowley, J. I.; Rapoport, H. *Acc. Chem. Res.* **1976**, *9*, 135.

(3) (a) Gerlach, M.; Jördens, F.; Kuhn, H.; Neumann, W. P.; Peterseim, M. *J. Org. Chem.* **1991**, *56*, 971. (b) Blanton, J. R.; Salley, J. M. *J. Org. Chem.* **1991**, *56*, 490.

(4) Merrifield, R. B. *J. Am. Chem. Soc.* **1963**, *85*, 2149.

(5) Schore, N. E.; Najdi, S. D. *J. Am. Chem. Soc.* **1990**, *112*, 441.

(6) Kurth, M. J.; Rodriguez, M. J. *J. Am. Chem. Soc.* **1987**, *109*, 7577.

(7) O'Hagan, D. *Nat. Prod. Rep.* **1989**, *6*, 205.

(8) Boivin, T. L. B. *Tetrahedron* **1987**, *43*, 3309.

(9) Kurth, M. J.; Rodriguez, M. J.; Olmstead, M. M. *J. Org. Chem.* **1990**, *55*, 283.

(10) Dupas, G.; Decormeille, A.; Bourguignon, J.; Queguiner, G. *Tetrahedron* **1989**, *45*, 2579.